horticulturae

MDPI

Article

Functional Characterization of Rose ABC Transporters Identifies *RcABCG5/50/59* as Candidate Genes Associated with *Botrytis cinerea* Resistance

Xiaoqian Cao [1], Meng Chen [1], Zicheng Wang [1], Hanyu Zhang [1], Xintong Liu [2,*] and Zhao Zhang [1,*]

[1] Beijing Key Laboratory of Development and Quality Control of Ornamental Crops, Department of Ornamental Horticulture, China Agricultural University, Beijing 100193, China; caoxiaoqian08@163.com (X.C.)
[2] Institute of Leisure Agriculture, Jiangsu Academy of Agricultural Sciences, Nanjing 210014, China
* Correspondence: lxtong17@163.com (X.L.); zhangzhao@cau.edu.cn (Z.Z.); Tel.: +86-10-62733603 (Z.Z.)

Abstract

Gray mold caused by *Botrytis cinerea* severely limits the postharvest quality of rose, but the contribution of ATP-binding cassette (ABC) transporters to rose defense remains unclear. Here, we identified 185 *RcABC* genes in the *Rosa chinensis* genome and classified them into eight subfamilies, with RcABCG as the largest subfamily. DESeq2-based RNA-seq analysis identified 13 significantly upregulated *RcABC* genes in response to *B. cinerea* infection at 48 hpi, nine of which belonged to the RcABCG subfamily. At 48 hpi, the $\log_2$ fold changes of these induced genes ranged from 1.34 to 7.98, and *RcABCG5*, *RcABCG50*, *RcABCG59*, and *RcABCG60* were selected for functional analysis. Further phylogenetic, gene-structure, and promoter analyses showed that several full-size *RcABCG* members were closely related to previously reported defense-associated ABCG transporters and harbored predicted GA-, MeJA-, and ABA-responsive cis-elements. Virus-induced gene silencing reduced the relative transcript levels of *RcABCG5*, *RcABCG50*, *RcABCG59*, and *RcABCG60* to 22.8%, 17.9%, 35.2%, and 27.5% of the TRV-GFP control, respectively. Mean lesion area increased from 39.27 mm^2 in TRV-GFP discs to 44.96, 46.95, and 43.23 mm^2 in *RcABCG5-*, *RcABCG50-*, and *RcABCG59*-silenced discs, respectively, whereas no significant lesion increase was observed in *RcABCG60*-silenced discs. Together, these results establish a genome-wide framework for defense-related ABC transporters in rose and identify *RcABCG5/50/59* as candidate genes associated with gray mold resistance under VIGS conditions.

Keywords: ATP-binding cassette transporters; ABCG; *B. cinerea*; *Rosa chinensis*; gray mold

Academic Editor: Jiafu Jiang

Received: 11 June 2026
Revised: 14 July 2026
Accepted: 15 July 2026
Published: 17 July 2026

1. Introduction

ATP-binding cassette (ABC) transporters constitute one of the largest membrane protein families in plants and mediate the translocation of diverse substrates across biological membranes [1]. Canonical ABC transporters contain highly conserved nucleotide-binding domains (NBDs) and variable transmembrane domains (TMDs), which together determine ATP-dependent transport activity and substrate specificity [2]. The NBD is the signature structural domain of ABC transporter proteins, which is very conserved and contains five characteristic sequences: the Walker A motif [GX4GK(ST)], Walker B motif [(RK)X3GX3L((hydrophobic)3)], ABC signature motif (also known as the Walker C motif [(LIVMFY)S(SG)GX3(RKA)(LIVMYA)X(LIVMF)(AG)], located between Walker A and Walker B), the H loop, and the Q loop [3]. In contrast, the TMD exhibits high variability and facilitates the transport of numerous substrates, including hormones, pigments, toxic

chemicals, defense-related secondary metabolites, lipid molecules, and reactive oxygen species (ROS)-related compounds [4]. According to the different combinations of NBDs and TMDs, transport proteins are classified into full-size proteins possessing two NBDs and two TMDs, half-size proteins containing one NBD and one TMD, and quarter-size proteins harboring only NBDs [5,6]. Based on sequence similarity, phylogenetic relationships, and domain organization, the plant ABC transporter family is divided into eight subfamilies: ABCA, ABCB, ABCC, ABCD, ABCE, ABCF, ABCG, and ABCI [7].

ABC transporters display broad substrate specificity and fulfill critical roles in diverse physiological processes such as hormone transport, lipid metabolism, stomatal regulation, and stress responses [8–10]. Among these subfamilies, ABCG constitutes the largest group and comprises full-size proteins (Pleiotropic Drug Resistance proteins, PDRs) and half-size proteins (White-Brown Complex proteins, WBCs), both of which are particularly crucial for plant disease resistance [8,11–13]. Expression of multiple ABCG members is induced by pathogen infection, including *ABCG16*, *ABCG33*, *ABCG36*, *ABCG37*, and *ABCG40* [11,13,14]. Specifically, ABCG34 mediates the transport of the indole alkaloid camalexin in response to pathogen invasion [15], whereas ABCG36 not only transports bioactive products of the PEN2 pathway [16] and camalexin [17] but also participates in hormone transport [18]. Additionally, *AtABCG5* restricts pathogen invasion by regulating stomatal movement, while *OsABCG5* promotes subepidermal lignification through transporting lignin precursors, thereby establishing a physical defense barrier [19].

Rose (*Rosa* spp.) represents a popular ornamental flower, which is known for its rich flower color, diverse flower types and long flowering period [20]. Rose symbolizes profound cultural meanings and serves as an indispensable element in both landscape design and daily life. However, gray mold caused by *Botrytis cinerea* has emerged as the most severe postharvest disease affecting roses, substantially diminishing their ornamental and commercial value and being figuratively termed the postharvest "cancer" of cut rose flowers [21]. Currently, ABC genes associated with rose resistance to gray mold remain unidentified. Although ABC transport proteins have been demonstrated to fulfill important roles in pathogen defense in other plant species [22], comprehensive investigation is still required to elucidate the specific functions and mechanisms underlying gray mold resistance in roses. Advances in this research area will enhance our understanding of rose defense mechanisms and provide a theoretical foundation for developing more effective disease management strategies to mitigate the impact of gray mold on rose ornamental quality.

To address this gap and to support the development of genetic resources for gray mold resistance in rose, we aimed to systematically characterize the ABC transporter family in *R. chinensis*. We performed genome-wide identification and classification of *RcABC* genes, followed by analyses of chromosomal distribution, duplication patterns, phylogenetic relationships, gene structures, conserved motifs, promoter cis-elements, and *B. cinerea*-responsive expression profiles. Selected *RcABCG* candidates were then functionally evaluated using virus-induced gene silencing (VIGS). We hypothesized that *Botrytis*-induced *RcABCG* transporters may participate in rose defense against gray mold. This study is expected to provide a basis for investigating ABC transporter-mediated disease resistance and for future molecular improvement of postharvest disease resistance in rose.

2. Materials and Methods

2.1. Identification and Characteristics of RcABC Transporter Genes in Rose Genome

Arabidopsis ABC transporter protein sequences were retrieved from TAIR/Araport11 (https://www.arabidopsis.org, accessed on 14 July 2026) and used as reference queries. The genome assembly and annotation files of *R. chinensis* 'Old Blush' were obtained from the

INRA RchiOBHm-V2 resource (https://lipm-browsers.toulouse.inra.fr/pub/RchiOBHm-V2/, accessed on 14 July 2026) [23].

Candidate RcABC proteins were identified using both BLASTP and HMMER searches. BLASTP searches were performed against the rose protein database using BLAST+ v2.6.0, with Arabidopsis ABC proteins as queries and an E-value $< 1 \times 10^{-5}$, sequence identity $\geq 30\%$, query coverage $\geq 50\%$, and a maximum of 20 target hits retained for each query. In parallel, hidden Markov model profiles of the conserved ABC_trans domain (PF00005.29) and ABC_membrane domain (PF00664.25) were downloaded from Pfam (http://pfam.xfam.org/, accessed on 14 July 2026) and used to search the rose protein dataset using HMMER v3.3.2, with an E-value $< 1 \times 10^{-5}$. Candidate sequences obtained from BLASTP and HMM searches were merged and further validated using InterPro, CDD (NCBI), and Pfam (EMBL). Proteins lacking a recognizable ABC conserved domain were excluded.

Non-redundant *RcABC* genes were determined after merging identical protein sequences obtained from different searches and removing redundant transcript isoforms. When multiple transcript isoforms were annotated at the same genomic locus, only the longest protein isoform was retained. Candidates without recognizable ABC conserved domain support from Pfam, CDD, or InterPro were excluded. Full-size, half-size, and quarter-size ABC proteins were classified according to the number and organization of nucleotide-binding domains and transmembrane domains [24]. Members with recognizable nucleotide-binding domains but lacking predicted transmembrane domains were retained only when supported by conserved ABC domains. Because ABCE and ABCF proteins are generally soluble ABC proteins [25], the absence of transmembrane domains in these subfamilies was not considered unusual. However, short or atypical members from other subfamilies were interpreted cautiously as putative quarter-size, partial, or annotation-dependent ABC candidates.

2.2. Phylogenetic Analyses, Gene Structure, Conserved Motif, and Promoter Analysis

Protein sequences of *RcABC* genes and Arabidopsis ABC reference proteins were aligned using ClustalW implemented in MEGA 7.0 [26]. The alignment was performed with the following parameters: protein weight matrix, BLOSUM; gap opening penalty, 10; gap extension penalty, 0.1; and all other parameters kept at default settings. The resulting alignments were visually inspected before tree construction, and obviously poorly aligned terminal regions were removed when necessary.

For family-level classification of RcABC proteins, a phylogenetic tree containing 185 RcABC and 129 Arabidopsis ABC proteins was constructed in MEGA 7.0 using the Neighbor-Joining method [27]. The Poisson correction model was used to calculate evolutionary distances, and the reliability of each node was evaluated with 1000 bootstrap replicates. The Neighbor-Joining tree was used mainly for broad subfamily classification because of the large number of ABC family members included in the analysis.

For detailed analysis of the RcABCG subfamily, exon–intron structures were visualized using TBtools v2.056 based on the rose genome annotation file [28]. The phylogenetic tree of the RcABCG subfamily was reconstructed using IQ-TREE v2.2.2 with the Maximum-Likelihood method [29] and visualized using ChiPlot (https://www.chiplot.online/, accessed on 14 July 2026). The best-fit amino acid substitution model was automatically selected using ModelFinder implemented in IQ-TREE, and the LG + F + R5 model was selected for final tree construction. Branch support was estimated using 1000 ultrafast bootstrap replicates [30]. The Neighbor-Joining tree was used for broad family-level classification, whereas the Maximum-Likelihood method was used for higher-resolution phylogenetic analysis of the RcABCG subfamily.

Promoter sequences corresponding to the 2000 bp region upstream of the transcription start site of each *RcABCG* gene were extracted for cis-element analysis. This region was selected because it is commonly used to represent the proximal promoter region and to capture major cis-regulatory elements in plant gene-family studies. Cis-acting elements were predicted using the PlantCARE database (http://bioinformatics.psb.ugent.be/webtools/plantcare/html/, accessed on 14 July 2026) [31] and grouped into light-responsive, hormone-responsive, stress-responsive, growth/development-related, and other regulatory categories. All predicted cis-acting elements were retained for summary, and no additional frequency-based filtering was applied. Conserved motifs of *RcABCG* proteins were identified using MEME Suite 5.5.5 (http://meme-suite.org/tools/meme, accessed on 14 July 2026), with the maximum number of motifs set to 10 and motif lengths set to 50–100 amino acids [32]. Sequence logos of conserved ABC domains were generated using WebLogo3 (http://weblogo.threeplusone.com/, accessed on 14 July 2026).

2.3. Chromosome Distribution and Collinearity Analyses

Chromosomal positions of *RcABC* genes were extracted from the *R. chinensis* 'Old Blush' RchiOBHm-V2 genome annotation file and visualized using TBtools v2.056 [33]. To identify duplicated *RcABC* gene pairs and collinear relationships, BLASTP search was first performed using the complete rose protein dataset, with an E-value $< 1 \times 10^{-10}$. The BLASTP results and gene position file were used as input files for MCScanX [28] and ColinearScan [34]. Collinear blocks were identified with a minimum block size of five genes. For ColinearScan, microsynteny chains were detected with an E-value $< 1 \times 10^{-10}$ and a minimum block size of five.

Duplicated *RcABC* gene pairs located within the same collinear block were defined as segmentally duplicated gene pairs. Tandem duplicated *RcABC* genes were defined as homologous *RcABC* genes located on the same chromosome, separated by no more than one intervening gene, and showing sequence identity $\geq 70\%$ and alignment coverage $\geq 70\%$. Interchromosomal collinearity relationships were visualized using TBtools and Circos. Homologous *RcABC* gene pairs that did not satisfy the criteria for segmental or tandem duplication were not classified as duplicated gene pairs.

2.4. Calculation of Ratios of Non-Synonymous (Ka) to Synonymous (Ks) Nucleotide Substitutions

Duplicated *RcABC* gene pairs identified from the collinearity analysis were used for Ka/Ks analysis. Protein sequences were first aligned using MAFFT v7.505 with default parameters, and the resulting protein alignments were converted into codon alignments based on the corresponding CDS sequences using PAL2NAL v14. The codon alignments were then used to calculate nonsynonymous substitution rates (Ka), synonymous substitution rates (Ks), and Ka/Ks ratios using EasyCodeML v1.4 [33]. The Ka/Ks ratio was used to infer the selective pressure acting on duplicated *RcABC* gene pairs, with Ka/Ks < 1, Ka/Ks = 1, and Ka/Ks > 1 indicating purifying selection, neutral evolution, and positive selection, respectively.

2.5. Expression of RcABC Genes in Response to B. cinerea

RNA-Seq data of rose petals under *B. cinerea* infection are available from the National Center for Biotechnology Information (NCBI) database, under accession number PRJNA414570. The RNA-Seq material consists of rose petal slices collected at 30 hpi and 48 hpi, with three biological replicates for both infected and control treatments.

Raw paired-end reads were first assessed using FastQC v0.11.9. Adapter sequences, low-quality bases, and short reads were removed using fastp v0.23.2. Reads shorter than 50 bp after trimming were discarded, and other filtering parameters were kept at default settings. The resulting clean paired-end reads were aligned to the *R. chinensis* 'Old

Blush' reference genome RchiOBHm-V2 using HISAT2 v2.2.1 with the --dta option [35,36]. HISAT2 was run in paired-end mode. Only concordantly mapped read pairs were used for downstream analysis. Reads with multiple genomic alignments were handled according to the default HISAT2/StringTie strategy and were not manually reallocated. Transcript assembly and expression quantification were performed using StringTie v2.2.1 with the RchiOBHm-V2 genome annotation file as reference guidance [37]. StringTie was run in reference-guided mode with the -e and -B options to estimate the abundance of annotated transcripts and generate files for downstream count-matrix construction. FPKM and TPM values were generated for expression-profile visualization only and were not used for differential expression analysis. For differential expression analysis, gene-level raw count matrices were generated from the StringTie output using the prepDE.py script provided with StringTie. The count matrix was imported into R v4.2.2 and analyzed using DESeq2 v1.38.3 [38]. Genes with fewer than 10 total reads across all samples were removed before analysis. DESeq2 normalization was performed to correct for differences in sequencing depth among libraries. Differential expression was analyzed separately for *B. cinerea*-infected versus mock-treated samples at 30 hpi and 48 hpi using the design formula ~ treatment. *p* values were adjusted using the Benjamini–Hochberg method to control the false discovery rate. Genes with an adjusted *p* value < 0.05 and $|\log_2 \text{fold change}| \geq 1$ were considered significantly differentially expressed genes. Among the significantly differentially expressed *RcABC* genes, those with $\log_2$ fold change > 1 in infected samples were defined as infection-induced *RcABC* genes.

To validate the RNA-seq expression profiles of selected *RcABC* genes, real-time quantitative PCR (RT-qPCR) was performed. Briefly, 1 μg of total RNA was used for first-strand cDNA synthesis in a 20 μL reaction system using HiScript II Q Select RT SuperMix (Vazyme, Nanjing, China). RT-qPCR was conducted on a StepOnePlus Real-Time PCR System (Applied Biosystems, Carlsbad, California, USA) with ChamQ SYBR qPCR Master Mix (Vazyme, Nanjing, China). RcUBI2 was used as the internal reference gene [39], and relative expression levels were calculated using the $2^{-\Delta\Delta Ct}$ method. All primers used in this study are listed in Supplementary Table S1.

2.6. VIGS and B. cinerea Inoculation Assays

To construct the silencing vectors, gene-specific fragments were selected from the coding sequences and/or 3′ untranslated regions (3′ UTRs) of *RcABCG5/50/59/60*. A 231 bp coding-region fragment of *RcABCG5*, a 105 bp 3′ UTR fragment of *RcABCG50*, a 127 bp 3′ UTR fragment of *RcABCG59*, and a 193 bp fragment of *RcABCG60* containing 80 bp of coding sequence and 113 bp of 3′ UTR were used for vector construction. The 3′ UTR fragments of *RcABCG50* and *RcABCG59* were selected to distinguish them from their closely related homologs, *RcABCG51/52* and *RcABCG58*, respectively. The specificity of each fragment was examined by BLASTN against the *R. chinensis* 'Old Blush' genome/transcriptome sequences and the identified *RcABC* gene sequences. Fragments with substantial similarity to non-target *RcABC* genes were discarded, and only fragments showing high specificity to the corresponding target genes were cloned into the TRV2 vector. TRV-GFP was used as the negative control, as previously described [40]. VIGS was established as previously described [41]. In brief, flowering roses at stage 2 were used for petal disc preparation. In each independent experiment, five constructs were tested, including TRV-GFP and four TRV-*RcABCG* silencing constructs. Twenty flowers were used per experiment. After removing the outermost four petal whorls, petals from the following five whorls were collected, and three 15 mm discs were punched from each whorl, resulting in 15 discs per flower. To reduce variation among flowers and petal positions, all discs collected in the same experiment were pooled and randomly assigned to the five constructs, with at least

48 discs per construct. *Agrobacterium* cultures containing constructs expressing TRV1 and TRV2 were mixed in a 1:1 ratio and vacuum-infiltrated into the petal discs. After 6 d of TRV infection, the petal discs were inoculated with 2 µL of *B. cinerea* spore suspension at a concentration of 1×10^5 spores/mL. The inoculated petal discs were placed on 0.4% water agar under humid conditions, and disease symptoms were photographed at 60 hpi. Lesion areas of individual discs were measured using ImageJ1.48v. For each construct, at least 48 individual discs were analyzed in each independent experiment. The entire VIGS assay was independently repeated three times with similar results. Target gene silencing efficiency was determined by RT-qPCR. The statistical analysis is described in Section 2.7, and all primers are listed in Supplementary Table S1.

2.7. Statistical Analysis

Lesion area and RT-qPCR data are presented as mean ± standard deviation. For VIGS assays, each independent experiment included at least 48 petal discs per construct. Lesion areas were measured for each petal disc using ImageJ, and the individual disc values from the same independent experiment were used for statistical comparisons between TRV-GFP and each TRV-*RcABCG* treatment. The VIGS assay was independently repeated three times to confirm the reproducibility of the observed trends. For RT-qPCR analysis, three biological replicates and three technical replicates were used for each treatment. Significant differences between two groups were determined using Student's *t*-test. Differences were considered statistically significant at $p < 0.05$ and highly significant at $p < 0.01$.

3. Results

3.1. Identification and Phylogenetic Analysis of RcABC Genes in Rose

To identify ABC family genes in the rose genome, predictions were performed through BLASTP and HMM analysis targeting conserved domains (PF00005, PF00664), followed by validation using the InterPro database. This approach ultimately yielded 185 non-redundant ABC transporter genes. All of which contained the conserved ATP-binding domain (NBD). Based on domain composition, transporters were classified into full-size (71 members), half-size (63 members), and quarter-size (44 members) categories, with 7 exceptional members exhibiting atypical domain architectures.

Phylogenetic analysis of rose RcABC (185) and *Arabidopsis* AtABC (129) member protein sequences was conducted using the NJ method (Supplementary Figure S1). This analysis identified eight RcABC subfamilies (ABCA through ABCI, excluding ABCH), comprising 7, 49, 33, 3, 1, 9, 70, and 13 members, respectively. The ABCG subfamily was predominant (approximately 40%), while the ABCD and ABCE subfamilies accounted for lower proportions (1.62% and 1.08%, respectively). Each subfamily received robust bootstrap support, thereby confirming the validity of the classification. Protein sizes displayed considerable variation, ranging from the longest member RcABCA1 (1887 amino acids) to the shortest member RcABCG68 (114 amino acids), with an average length of 890 amino acids. Detailed characteristics of all identified genes are presented in Table 1.

Table 1. Members of the ABC gene family, as predicted in the rose genome sequence.

Accession Number [a]	Gene	Sub [b]	AA [c]	TMD	NBD	CDS (bp)	Exon	Intron
RchiOBHmChr3g0482761	*RcABCA1*	A	1887	2	2	5664	40	39
RchiOBHmChr5g0061021	*RcABCA2*	A	988	1	1	2967	15	14
RchiOBHmChr7g0178831	*RcABCA3*	A	942	1	1	2829	18	17
RchiOBHmChr7g0178841	*RcABCA4*	A	970	1	1	2913	14	13
RchiOBHmChr7g0180781	*RcABCA5*	A	907	1	1	2724	15	14

Table 1. *Cont.*

Accession Number [a]	Gene	Sub [b]	AA [c]	TMD	NBD	CDS (bp)	Exon	Intron
RchiOBHmChr7g0180791	*RcABCA6*	A	962	1	1	2889	18	17
RchiOBHmChr7g0180811	*RcABCA7*	A	937	1	1	2814	18	17
RchiOBHmChr1g0365761	*RcABCB1*	B	1409	2	2	4230	11	10
RchiOBHmChr1g0376591	*RcABCB2*	B	716	1	1	2151	16	15
RchiOBHmChr1g0383351	*RcABCB3*	B	1270	2	2	3813	9	8
RchiOBHmChr2g0091821	*RcABCB4*	B	1246	2	2	3741	9	8
RchiOBHmChr2g0146391	*RcABCB5*	B	154	0	1	465	2	1
RchiOBHmChr2g0146621	*RcABCB6*	B	1513	2	2	4542	9	8
RchiOBHmChr2g0168761	*RcABCB7*	B	1250	2	2	3753	10	9
RchiOBHmChr2g0169781	*RcABCB8*	B	519	1	1	1560	5	4
RchiOBHmChr2g0169791	*RcABCB9*	B	250	1	1	753	1	0
RchiOBHmChr2g0169801	*RcABCB10*	B	127	0	1	384	1	0
RchiOBHmChr2g0169841	*RcABCB11*	B	1252	2	2	3759	7	6
RchiOBHmChr2g0169851	*RcABCB12*	B	590	1	2	1773	3	2
RchiOBHmChr2g0169861	*RcABCB13*	B	136	0	1	411	2	1
RchiOBHmChr2g0173091	*RcABCB14*	B	679	1	1	2040	18	17
RchiOBHmChr3g0448061	*RcABCB15*	B	1260	2	2	3783	12	11
RchiOBHmChr3g0470311	*RcABCB16*	B	1347	2	2	4044	10	9
RchiOBHmChr3g0474221	*RcABCB17*	B	644	1	1	1935	5	4
RchiOBHmChr3g0474231	*RcABCB18*	B	601	1	1	1806	7	6
RchiOBHmChr3g0479341	*RcABCB19*	B	533	1	1	1602	6	5
RchiOBHmChr3g0479351	*RcABCB20*	B	497	1	1	1494	8	7
RchiOBHmChr3g0485931	*RcABCB21*	B	1295	2	2	3888	12	11
RchiOBHmChr3g0485961	*RcABCB22*	B	1295	2	2	3888	12	11
RchiOBHmChr4g0410931	*RcABCB23*	B	450	1	1	1353	7	6
RchiOBHmChr4g0427151	*RcABCB24*	B	1290	2	2	3873	12	11
RchiOBHmChr4g0427161	*RcABCB25*	B	1286	2	2	3861	12	11
RchiOBHmChr4g0427211	*RcABCB26*	B	230	0	1	693	4	3
RchiOBHmChr4g0427241	*RcABCB27*	B	1285	2	2	3858	12	11
RchiOBHmChr4g0427271	*RcABCB28*	B	1316	2	2	3951	11	10
RchiOBHmChr4g0427711	*RcABCB29*	B	1284	2	2	3855	12	11
RchiOBHmChr4g0427721	*RcABCB30*	B	1301	2	2	3906	12	11
RchiOBHmChr4g0427771	*RcABCB31*	B	321	0	1	966	4	3
RchiOBHmChr4g0427781	*RcABCB32*	B	491	1	1	1476	5	4
RchiOBHmChr4g0427791	*RcABCB33*	B	1284	2	2	3855	12	11
RchiOBHmChr4g0427851	*RcABCB34*	B	1311	2	2	3936	11	10
RchiOBHmChr4g0427861	*RcABCB35*	B	1387	2	2	4164	12	11
RchiOBHmChr4g0432491	*RcABCB36*	B	331	1	1	996	3	2
RchiOBHmChr4g0432501	*RcABCB37*	B	1263	2	2	3792	7	6
RchiOBHmChr4g0432941	*RcABCB38*	B	706	1	1	2121	18	17
RchiOBHmChr5g0012641	*RcABCB39*	B	1266	2	2	3801	12	11
RchiOBHmChr5g0015481	*RcABCB40*	B	298	1	1	897	8	7
RchiOBHmChr5g0037461	*RcABCB41*	B	837	1	1	2514	2	1
RchiOBHmChr5g0037681	*RcABCB42*	B	926	2	1	2781	6	5
RchiOBHmChr5g0037691	*RcABCB43*	B	289	0	1	870	2	1
RchiOBHmChr5g0073901	*RcABCB44*	B	718	1	1	2157	18	17
RchiOBHmChr6g0303231	*RcABCB45*	B	172	0	1	519	1	0
RchiOBHmChr6g0303241	*RcABCB46*	B	124	0	1	375	1	0
RchiOBHmChr6g0303261	*RcABCB47*	B	352	1	1	1059	8	7
RchiOBHmChr6g0303281	*RcABCB48*	B	433	1	1	1302	3	2
RchiOBHmChr7g0210291	*RcABCB49*	B	1263	2	2	3792	12	11
RchiOBHmChr1g0321081	*RcABCC1*	C	270	0	1	813	4	3
RchiOBHmChr1g0340111	*RcABCC2*	C	1470	2	2	4413	11	10
RchiOBHmChr1g0340151	*RcABCC3*	C	1515	2	2	4548	11	10
RchiOBHmChr1g0379781	*RcABCC4*	C	181	0	1	546	2	1
RchiOBHmChr2g0132931	*RcABCC5*	C	1440	2	2	4323	35	34
RchiOBHmChr2g0142721	*RcABCC6*	C	1293	2	2	3882	12	11
RchiOBHmChr2g0142761	*RcABCC7*	C	1473	2	2	4422	12	11

Table 1. *Cont.*

Accession Number [a]	Gene	Sub [b]	AA [c]	TMD	NBD	CDS (bp)	Exon	Intron
RchiOBHmChr2g0142771	*RcABCC8*	C	1467	2	2	4404	12	11
RchiOBHmChr2g0150061	*RcABCC9*	C	884	1	2	2655	11	10
RchiOBHmChr4g0406401	*RcABCC10*	C	1502	2	2	4509	10	9
RchiOBHmChr4g0406811	*RcABCC11*	C	1509	2	2	4530	10	9
RchiOBHmChr4g0431141	*RcABCC12*	C	1474	2	2	4425	10	9
RchiOBHmChr4g0431381	*RcABCC13*	C	704	1	2	2115	9	8
RchiOBHmChr4g0431391	*RcABCC14*	C	177	0	1	534	1	0
RchiOBHmChr4g0431551	*RcABCC15*	C	1474	2	2	4425	10	9
RchiOBHmChr4g0431711	*RcABCC16*	C	1449	2	2	4350	11	10
RchiOBHmChr4g0435371	*RcABCC17*	C	252	1	1	759	7	6
RchiOBHmChr5g0015421	*RcABCC18*	C	1630	2	2	4893	29	28
RchiOBHmChr5g0015441	*RcABCC19*	C	1509	2	2	4530	26	25
RchiOBHmChr5g0015451	*RcABCC20*	C	1644	2	2	4935	26	25
RchiOBHmChr5g0015491	*RcABCC21*	C	761	1	1	2286	9	8
RchiOBHmChr5g0037451	*RcABCC22*	C	665	1	1	1998	8	7
RchiOBHmChr5g0046661	*RcABCC23*	C	1441	2	2	4326	11	10
RchiOBHmChr5g0046671	*RcABCC24*	C	1480	2	2	4443	11	10
RchiOBHmChr5g0046681	*RcABCC25*	C	1509	2	2	4530	10	9
RchiOBHmChr6g0286471	*RcABCC26*	C	1542	2	2	4629	11	10
RchiOBHmChr6g0293781	*RcABCC27*	C	1510	2	2	4533	12	11
RchiOBHmChr6g0306331	*RcABCC28*	C	1556	2	2	4671	11	10
RchiOBHmChr7g0195711	*RcABCC29*	C	1486	2	2	4461	12	11
RchiOBHmChr7g0195721	*RcABCC30*	C	1489	2	2	4470	11	10
RchiOBHmChr7g0195751	*RcABCC31*	C	1243	2	2	3732	11	10
RchiOBHmChr7g0195781	*RcABCC32*	C	1237	2	2	3714	12	11
RchiOBHmChr7g0195801	*RcABCC33*	C	1443	2	2	4332	13	12
RchiOBHmChr2g0171001	*RcABCD1*	D	293	1	1	882	7	6
RchiOBHmChr3g0484971	*RcABCD2*	D	1343	2	2	4032	27	26
RchiOBHmChr5g0022531	*RcABCD3*	D	749	1	1	2250	10	9
RchiOBHmChr6g0304351	*RcABCE*	E	340	0	1	1023	8	7
RchiOBHmChr2g0116631	*RcABCF1*	F	716	0	2	2151	9	8
RchiOBHmChr2g0116661	*RcABCF2*	F	479	0	2	1440	8	7
RchiOBHmChr2g0116701	*RcABCF3*	F	115	0	1	348	3	2
RchiOBHmChr2g0116821	*RcABCF4*	F	234	0	1	705	2	1
RchiOBHmChr2g0116831	*RcABCF5*	F	116	0	1	351	3	2
RchiOBHmChr2g0149831	*RcABCF6*	F	716	0	2	2151	2	1
RchiOBHmChr5g0057741	*RcABCF7*	F	597	0	2	1794	6	5
RchiOBHmChr6g0306241	*RcABCF8*	F	699	0	2	2100	1	0
RchiOBHmChr7g0186321	*RcABCF9*	F	712	0	2	2139	18	17
RchiOBHmChr1g0332261	*RcABCG1*	G	299	0	1	900	2	1
RchiOBHmChr1g0362891	*RcABCG2*	G	1116	0	1	3351	14	13
RchiOBHmChr1g0365031	*RcABCG3*	G	748	1	1	2247	1	0
RchiOBHmChr1g0378951	*RcABCG4*	G	654	1	1	1965	1	0
RchiOBHmChr2g0089741	*RcABCG5*	G	1421	2	2	4266	24	23
RchiOBHmChr2g0112551	*RcABCG6*	G	687	1	1	2064	7	6
RchiOBHmChr2g0112561	*RcABCG7*	G	464	0	1	1395	6	5
RchiOBHmChr2g0112631	*RcABCG8*	G	709	1	1	2130	8	7
RchiOBHmChr2g0112641	*RcABCG9*	G	708	1	1	2127	8	7
RchiOBHmChr2g0121921	*RcABCG10*	G	460	1	1	1383	2	1
RchiOBHmChr2g0129131	*RcABCG11*	G	611	1	1	1836	1	0
RchiOBHmChr2g0137121	*RcABCG12*	G	1422	2	2	4269	24	23
RchiOBHmChr2g0140401	*RcABCG13*	G	1491	2	2	4476	21	20
RchiOBHmChr2g0140691	*RcABCG14*	G	1105	0	1	3318	14	13
RchiOBHmChr2g0140701	*RcABCG15*	G	1111	0	1	3336	14	13
RchiOBHmChr2g0153091	*RcABCG16*	G	699	1	1	2100	8	7
RchiOBHmChr2g0153111	*RcABCG17*	G	706	1	1	2121	8	7
RchiOBHmChr2g0153141	*RcABCG18*	G	717	1	1	2154	8	7
RchiOBHmChr2g0153161	*RcABCG19*	G	440	0	1	1323	6	5
RchiOBHmChr2g0169331	*RcABCG20*	G	1313	2	2	3942	20	19

Table 1. *Cont.*

Accession Number [a]	Gene	Sub [b]	AA [c]	TMD	NBD	CDS (bp)	Exon	Intron
RchiOBHmChr2g0169361	*RcABCG21*	G	1390	2	2	4173	24	23
RchiOBHmChr2g0169371	*RcABCG22*	G	781	1	1	2346	13	12
RchiOBHmChr2g0169381	*RcABCG23*	G	640	1	1	1923	8	7
RchiOBHmChr2g0169401	*RcABCG24*	G	430	0	1	1293	7	6
RchiOBHmChr2g0169411	*RcABCG25*	G	1032	2	1	3099	16	15
RchiOBHmChr3g0456491	*RcABCG26*	G	706	1	1	2121	10	9
RchiOBHmChr3g0458321	*RcABCG27*	G	1443	2	2	4332	24	23
RchiOBHmChr3g0467991	*RcABCG28*	G	737	1	1	2214	2	1
RchiOBHmChr3g0469991	*RcABCG29*	G	1138	0	1	3417	14	13
RchiOBHmChr3g0472451	*RcABCG30*	G	1449	2	2	4350	20	19
RchiOBHmChr3g0477391	*RcABCG31*	G	697	1	1	2094	11	10
RchiOBHmChr3g0482931	*RcABCG32*	G	630	1	1	1893	8	7
RchiOBHmChr3g0493261	*RcABCG33*	G	824	1	1	2475	4	3
RchiOBHmChr4g0427141	*RcABCG34*	G	1428	2	2	4287	24	23
RchiOBHmChr4g0427321	*RcABCG35*	G	1483	2	2	4452	23	22
RchiOBHmChr4g0436231	*RcABCG36*	G	692	1	1	2079	5	4
RchiOBHmChr4g0440941	*RcABCG37*	G	821	1	1	2466	12	11
RchiOBHmChr4g0441011	*RcABCG38*	G	860	2	1	2583	13	12
RchiOBHmChr4g0441021	*RcABCG39*	G	438	0	1	1317	8	7
RchiOBHmChr5g0011781	*RcABCG40*	G	682	2	1	2049	3	2
RchiOBHmChr5g0031401	*RcABCG41*	G	610	1	1	1833	1	0
RchiOBHmChr5g0034741	*RcABCG42*	G	618	1	1	1857	4	3
RchiOBHmChr5g0052851	*RcABCG43*	G	406	1	1	1221	6	5
RchiOBHmChr5g0052971	*RcABCG44*	G	701	1	1	2106	9	8
RchiOBHmChr5g0053001	*RcABCG45*	G	678	1	1	2037	9	8
RchiOBHmChr5g0053511	*RcABCG46*	G	638	1	1	1917	4	3
RchiOBHmChr5g0053631	*RcABCG47*	G	629	1	1	1890	4	3
RchiOBHmChr5g0055051	*RcABCG48*	G	1452	2	2	4359	20	19
RchiOBHmChr5g0055091	*RcABCG49*	G	1441	2	2	4326	20	19
RchiOBHmChr5g0055111	*RcABCG50*	G	1441	2	2	4326	20	19
RchiOBHmChr5g0055121	*RcABCG51*	G	1445	2	2	4338	20	19
RchiOBHmChr5g0055131	*RcABCG52*	G	1454	2	2	4365	20	19
RchiOBHmChr5g0057821	*RcABCG53*	G	723	1	1	2172	12	11
RchiOBHmChr5g0058181	*RcABCG54*	G	1124	0	1	3375	14	13
RchiOBHmChr5g0069411	*RcABCG55*	G	1421	2	2	4266	19	18
RchiOBHmChr5g0075901	*RcABCG56*	G	688	1	1	2067	9	8
RchiOBHmChr6g0276641	*RcABCG57*	G	658	1	1	1977	12	11
RchiOBHmChr6g0286071	*RcABCG58*	G	1399	2	2	4200	23	22
RchiOBHmChr6g0286401	*RcABCG59*	G	1426	2	2	4281	25	24
RchiOBHmChr6g0298851	*RcABCG60*	G	1451	2	2	4356	23	22
RchiOBHmChr6g0298871	*RcABCG61*	G	836	1	2	2511	17	16
RchiOBHmChr6g0298901	*RcABCG62*	G	1317	2	2	3954	22	21
RchiOBHmChr6g0298911	*RcABCG63*	G	1421	2	2	4266	24	23
RchiOBHmChr6g0304401	*RcABCG64*	G	660	1	1	1983	4	3
RchiOBHmChr7g0178121	*RcABCG65*	G	832	1	1	2499	4	3
RchiOBHmChr7g0201801	*RcABCG66*	G	1398	2	2	4197	22	21
RchiOBHmChr7g0211531	*RcABCG67*	G	1407	2	2	4224	21	20
RchiOBHmChr7g0218751	*RcABCG68*	G	114	0	1	345	1	0
RchiOBHmChr7g0221691	*RcABCG69*	G	739	1	1	2220	3	2
RchiOBHmChr7g0221951	*RcABCG70*	G	658	1	1	1977	1	0
RchiOBHmChr1g0382991	*RcABCI1*	I	138	0	1	417	3	2
RchiOBHmChr2g0086001	*RcABCI2*	I	228	0	1	687	2	1
RchiOBHmChr2g0175931	*RcABCI3*	I	275	0	1	828	10	9
RchiOBHmChr3g0448111	*RcABCI4*	I	343	0	1	1032	10	9
RchiOBHmChr3g0457711	*RcABCI5*	I	318	0	1	957	3	2
RchiOBHmChr4g0398581	*RcABCI6*	I	273	0	1	822	4	3
RchiOBHmChr5g0037441	*RcABCI7*	I	462	1	1	1389	4	3
RchiOBHmChr6g0244501	*RcABCI8*	I	332	0	1	999	5	4
RchiOBHmChr6g0287691	*RcABCI9*	I	283	0	1	852	6	5

Table 1. *Cont.*

Accession Number [a]	Gene	Sub [b]	AA [c]	TMD	NBD	CDS (bp)	Exon	Intron
RchiOBHmChr6g0304361	*RcABCI10*	I	251	0	1	756	5	4
RchiOBHmChr7g0218741	*RcABCI11*	I	173	0	1	522	4	3
RchiOBHmChr7g0220961	*RcABCI12*	I	271	0	1	816	7	6
RchiOBHmChr7g0234131	*RcABCI13*	I	190	0	1	573	2	1

[a] Available at https://lipm-browsers.toulouse.inra.fr/pub/RchiOBHm-V2/, accessed on 14 July 2026; [b] Subfamily; [c] Amino Acids.

Furthermore, domain analysis showed that RcABC proteins possessed three highly conserved domains (Supplementary Figure S2b): Walker A (positions 10–20), Walker B (positions 140–152), and signature C motif (positions 127–140). These conserved motifs were also observed in Arabidopsis AtABC proteins (Supplementary Figure S2a).

3.2. Chromosomal Locations, Gene Duplication and Microsynteny Analysis

The 185 *RcABC* genes were unevenly distributed across the seven rose chromosomes (Figure 1). Chromosome 2 harbored the largest number of genes (46 members), followed by chromosome 5 (35 members) and chromosome 4 (31 members), whereas chromosome 1 contained the fewest (12 members) genes. The distribution of *RcABC* genes differed among chromosomes. Several genes on chromosomes 4 and 6 were enriched at distal chromosomal regions, while most others clustered within specific localized areas. The eight subfamilies demonstrated non-uniform distribution patterns, with the ABCG subfamily (the largest group) being predominantly localized on chromosomes 2 and 5 (collectively accounting for 54% of ABCG members). The ABCB subfamily (the second largest group) was mainly positioned on chromosomes 2 and 4 (representing 55% of ABCB members), whereas the ABCA subfamily was primarily concentrated on chromosome 7.

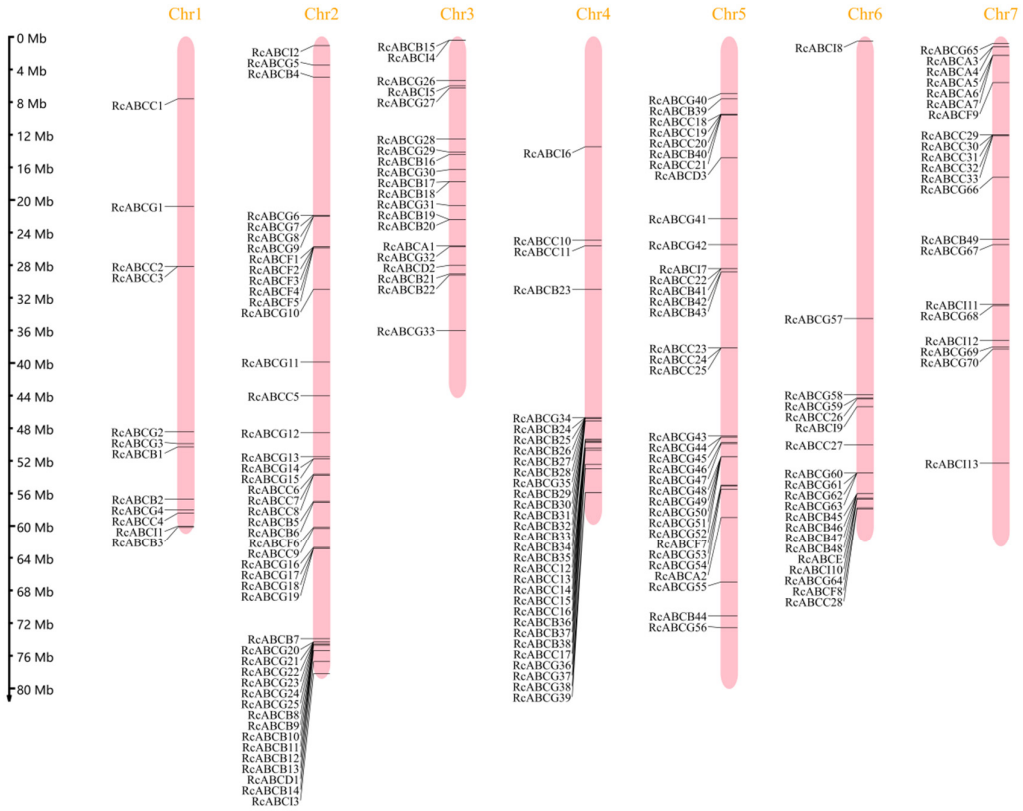

Figure 1. Chromosomal distribution of the *RcABC* genes. The physical location of each *RcABC* gene is listed on the seven chromosomes of *R. chinensis*. Chr1–7 represents chromosome numbers 1–7.

Gene duplication events within the *RcABC* family were further investigated, showing seven duplicated gene pairs that exclusively belonged to the ABCG subfamily (Figure 2). These duplicated gene pairs were classified as segmentally duplicated pairs because they were located on different chromosomes. Notably, *RcABCG2* located on chromosome 1 underwent independent segmental duplication events with both *RcABCG29* on chromosome 3 and RcABCG54 on chromosome 5. Comprehensive microsynteny relationships among *RcABC* genes across chromosomes are illustrated in Figure 2.

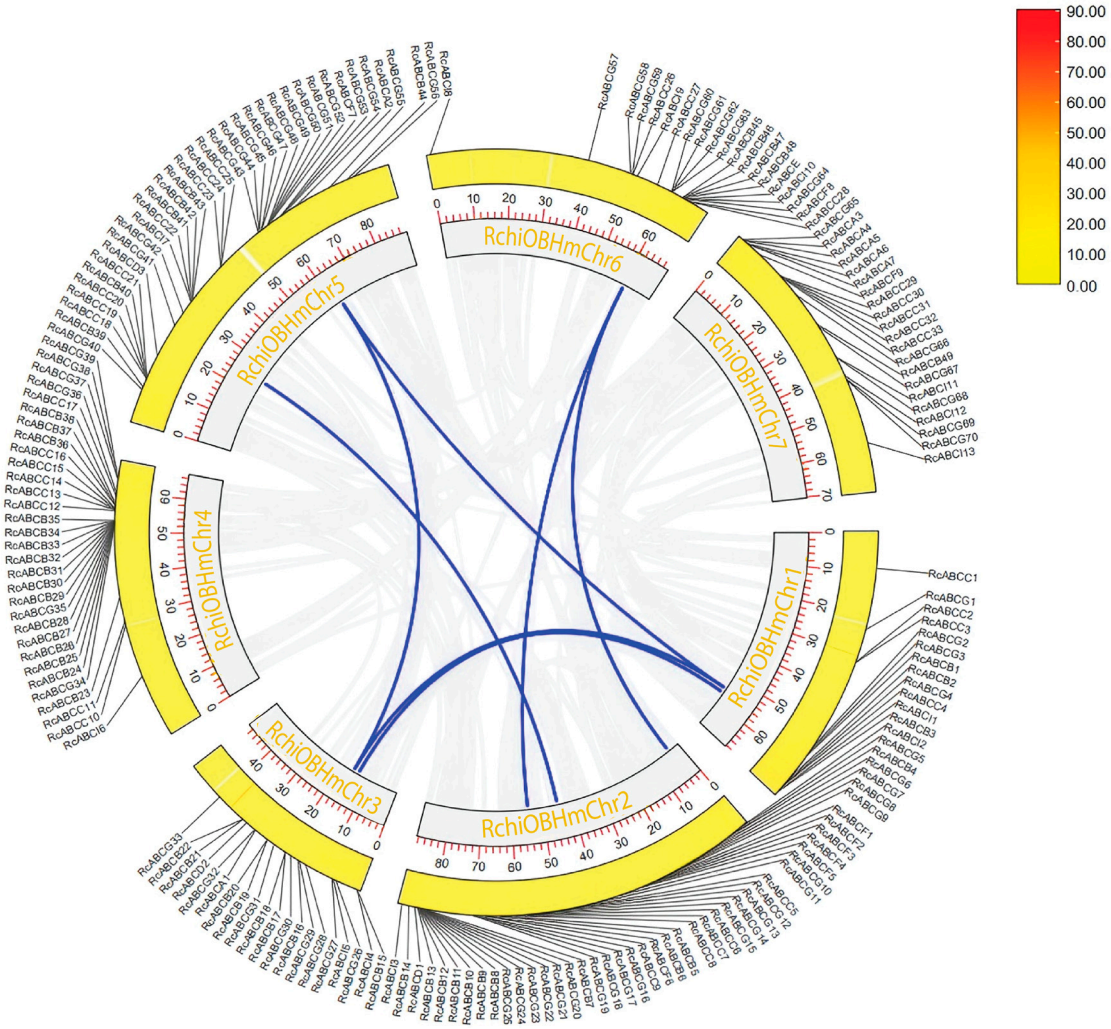

Figure 2. Microsyntenic analyses of the rose ABC super protein family in the *R. chinensis* genome. Circular visualization of rose ABC protein family members is mapped onto different chromosomes using Circosv0.69-9. The blue lines indicate rose ABC genes with a syntenic relationship. The grey lines represent all syntenic blocks in the genome of *R. chinensis*.

To evaluate selective constraints on duplicated *RcABC* genes, the Ka and Ks were calculated for each duplicated gene pair, and their ratio (Ka/Ks) was subsequently determined for evolutionary analysis (Table 2). It is well-known that Ka/Ks > 1 indicates positive selection, while Ka/Ks < 1 indicates purifying selection. Ka/Ks values were successfully estimated for six of the seven duplicated *RcABCG* gene pairs and ranged from 0.110 to 0.223, all below 1, suggesting purifying selection. The RcABCG5/RcABCG63 pair showed an undefined Ks value, likely due to synonymous-site saturation, and was therefore excluded from Ka/Ks-based selection inference.

Table 2. Duplication analysis of the ABC gene family.

Seq1	Seq2	Ka (dN)	Ks (dS)	Ka/Ks (ω)	S Sites	N Sites	Effective Len
RcABCG2	*RcABCG29*	0.277108	1.242445	0.223035	776.75	2523.25	3300
RcABCG3	*RcABCG28*	0.23296	2.111631	0.110322	534.916667	1652.083333	2187
RcABCG2	*RcABCG54*	0.259142	1.413152	0.183378	766.333333	2503.666667	3270
RcABCG11	*RcABCG41*	0.254556	1.482479	0.17171	424.083333	1375.916667	1800
RcABCG5	*RcABCG63*	0.314687	NA	NA	996.083333	3212.916667	4209
RcABCG12	*RcABCG60*	0.185058	1.660043	0.111478	997.75	3259.25	4257
RcABCG29	*RcABCG54*	0.284513	1.319061	0.215693	774.666667	2513.333333	3288

NA indicates that Ks and Ka/Ks could not be reliably estimated because of synonymous-site saturation/high sequence divergence (pS $\geq$ 0.75).

3.3. The Expression of RcABC Genes in Response to B. cinerea Infection

To investigate the expression patterns of *RcABC* genes in response to *B. cinerea* infection, DESeq2-based differential expression analysis was performed using RNA-seq data from rose petals collected at 30 hpi and 48 hpi. The 13 *RcABC* genes, including *RcABCB11*, *RcABCB29*, *RcABCB30*, *RcABCC2*, *RcABCG5*, *RcABCG6*, *RcABCG29*, *RcABCG50*, *RcABCG51*, *RcABCG52*, *RcABCG58*, *RcABCG59*, and *RcABCG60*, showed increased expression at 48 hpi (Table 3). Among these genes, eight also showed increased expression at 30 hpi. Notably, nine of the 13 infection-responsive *RcABC* genes belonged to the RcABCG subfamily, accounting for 69.23% of the responsive genes. Based on their expression profiles, subfamily classification, phylogenetic relationships, and promoter features, selected *RcABCG* genes were further analyzed in subsequent functional assays.

To validate the RNA-seq results, RT-qPCR was performed for selected infection-responsive *RcABCG* genes, including *RcABCG5*, *RcABCG50*, *RcABCG59*, and *RcABCG60*. RT-qPCR analysis showed that these genes were upregulated after *B. cinerea* infection compared with the mock-treated controls (Figure 3). The expression trends of *RcABCG5*, *RcABCG50*, *RcABCG59*, and *RcABCG60* were generally consistent with the RNA-seq profiles, especially at 48 hpi.

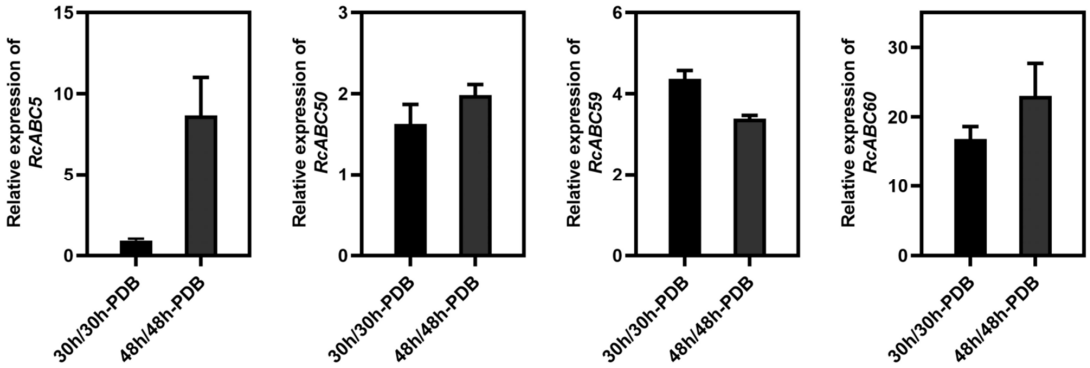

Figure 3. Validation of expression of selected *RcABCG* genes using qPCR at 30 and 48 h post inoculation. *RcUBI2* was used as a reference gene. The primers used for each transcript are listed in Table S1. PDB, potato dextrose broth. 'T' represents the standard deviation.

Table 3. Expression of the rose ABC genes under *B. cinerea* infection [a].

Accession Number	Gene [a]	Group	log_2FC 30 hpi (Adjusted *p* Value < 0.05)	log_2FC 48 hpi (Adjusted *p* Value < 0.05)
RchiOBHm_Chr2g0169841	*RcABCB11*	ABCB	-	6.14344
RchiOBHm_Chr4g0427711	*RcABCB29*	ABCB	2.35183	3.95003
RchiOBHm_Chr4g0427721	*RcABCB30*	ABCB	4.59797	5.22688
RchiOBHm_Chr1g0340111	***RcABCC2***	ABCC	1.22562	1.33914
RchiOBHm_Chr2g0089741	***RcABCG5***	ABCG	-	1.46865
RchiOBHm_Chr2g0112551	*RcABCG6*	ABCG	3.73972	4.91396

Table 3. *Cont.*

Accession Number	Gene [a]	Group	log_2FC 30 hpi (Adjusted p Value < 0.05)	log_2FC 48 hpi (Adjusted p Value < 0.05)
RchiOBHm_Chr3g0469991	***RcABCG29***	ABCG	-	4.67551
RchiOBHm_Chr5g0055111	*RcABCG50*	ABCG	2.42942	3.92323
RchiOBHm_Chr5g0055121	*RcABCG51*	ABCG	3.88137	4.39874
RchiOBHm_Chr5g0055131	*RcABCG52*	ABCG	3.14333	3.67407
RchiOBHm_Chr6g0286071	*RcABCG58*	ABCG	-	4.68104
RchiOBHm_Chr6g0286401	*RcABCG59*	ABCG	-	2.92895
RchiOBHm_Chr6g0298851	***RcABCG60***	ABCG	5.7242	7.97836

[a] Duplicated *RcABC* genes are shown in bold.

3.4. Phylogenetic Analysis of Rose ABCG Genes

To assess the evolutionary relationships among RcABCG proteins, Arabidopsis AtABCG proteins, and previously reported plant ABCG proteins associated with disease resistance, a phylogenetic tree was constructed using the Maximum-Likelihood method (Figure 4). The RcABCG proteins were grouped with their corresponding Arabidopsis ABCG members. Full-size RcABCG transporters clustered with PDR-type ABCG proteins, whereas half-size RcABCG transporters clustered with WBC-type ABCG proteins. Five quarter-size transporters, including RcABCG2, RcABCG14, RcABCG15, RcABCG29, and RcABCG54, formed an independent clade. These five genes included three of the seven duplicated gene pairs identified in the RcABC family. The remaining quarter-size RcABCG proteins were distributed in branches containing half-size ABCG transporters. Several previously characterized defense-associated ABCG proteins were located within branches containing full-size ABCG transporters.

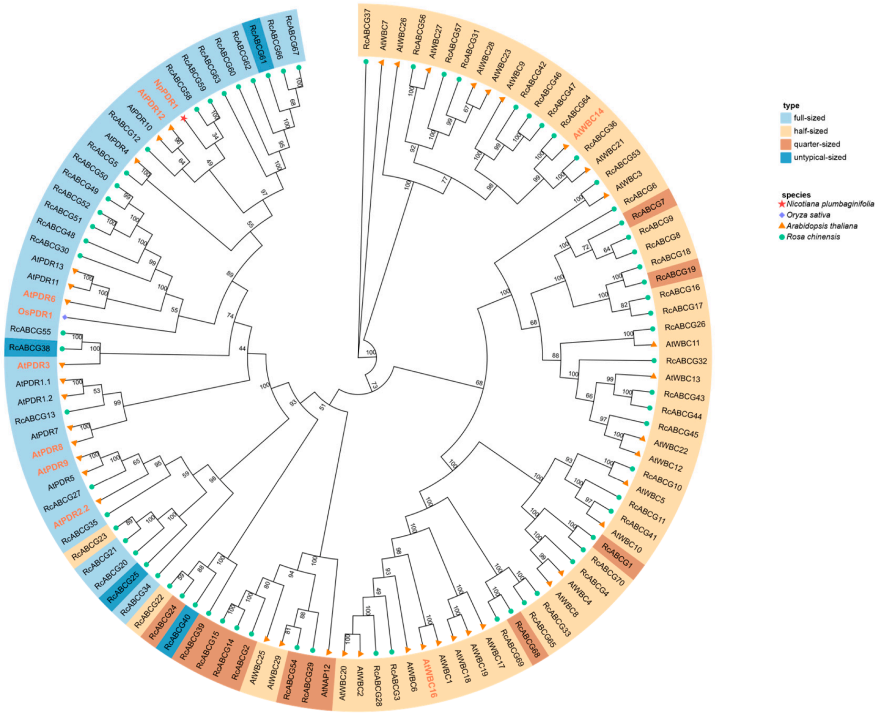

Figure 4. Phylogenetic analyses of ABCG protein subfamily in rose, Arabidopsis, and the disease-resistance-related ABCG protein subfamily from other plant species, including tobacco (*Nicotiana benthamiana*) and rice (*Oryza sativa*). The phylogenetic tree uses an IQ-tree with the maximum likelihood method. Numbers on the nodes of the branches represent bootstrap values. The ABCGs reported to be involved in plant disease resistance are marked in orange. Different groups are marked with different colors.

Exon–intron structure and conserved motif analyses were performed to further characterize the RcABCG subfamily (Figure 5). *RcABCG* genes with close phylogenetic relationships generally showed similar exon–intron structures. Conserved motif analysis showed differences in motif composition among full-size, half-size, quarter-size, and atypical *RcABCG* proteins. Full-size RcABCG proteins contained most of the identified motifs, except for RcABCG67 and RcABCG20. Motifs 2, 1, 3, and 8 were detected in most RcABCG proteins, whereas motifs 7, 10, 4, 9, and 5 were mainly present in full-size proteins. A total of 10 conserved motifs, with lengths ranging from 50 to 100 amino acids, were identified using MEME (Supplementary Table S2). Conserved domain prediction using NCBI-CDD showed differences in domain composition among RcABCG members (Figure 4).

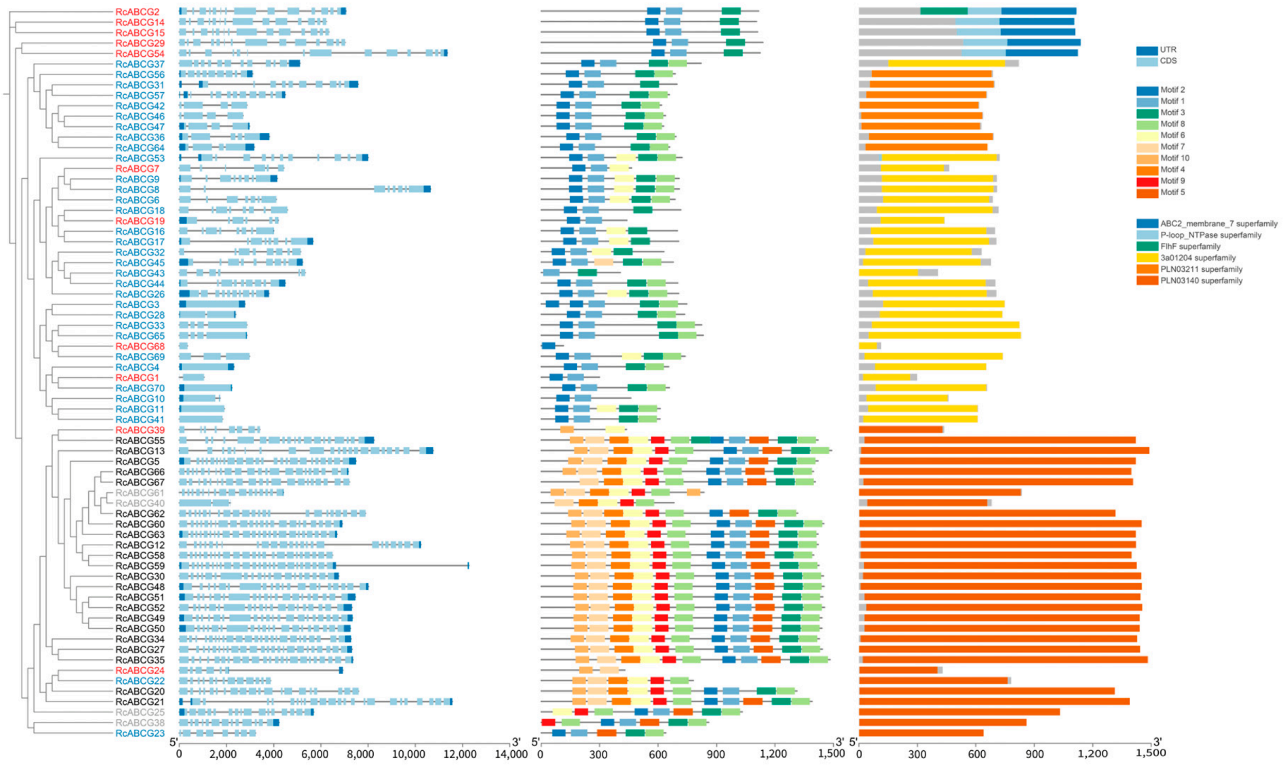

Figure 5. Gene structures and protein motifs of rose ABCG family genes. Exon–intron structure of RcABCGs is shown in the left part of the figure, and the blue boxes, light blue boxes, and gray lines represent UTRs, exons, and introns, respectively. Conserved domains of RcABCs are displayed in the middle part of the figure. The right part displays the visualization of CDD-predicted protein structure. The scale on the bottom is provided as a reference. The clustering is performed according to the results of phylogenetic analysis.

3.5. Analysis of Cis-Regulatory Elements in RcABCG Promoters

To characterize the potential regulatory features of the RcABCG subfamily, cis-acting elements in the 2000 bp upstream promoter regions of 70 *RcABCG* genes were predicted using the PlantCARE database (Figure 6). Multiple types of cis-acting elements were identified, including light-responsive, hormone-responsive, stress-responsive, growth/development-related, and transcription factor binding-related elements. Light-responsive elements were detected in most *RcABCG* promoters. Hormone-responsive elements were also widely distributed, including MeJA-, ABA-, and GA-responsive elements, which were present in 77%, 56%, and 44% of *RcABCG* genes, respectively. In addition, anaerobic induction-related elements and other stress-responsive elements were detected in 61% and 26% of *RcABCG* genes, respectively.

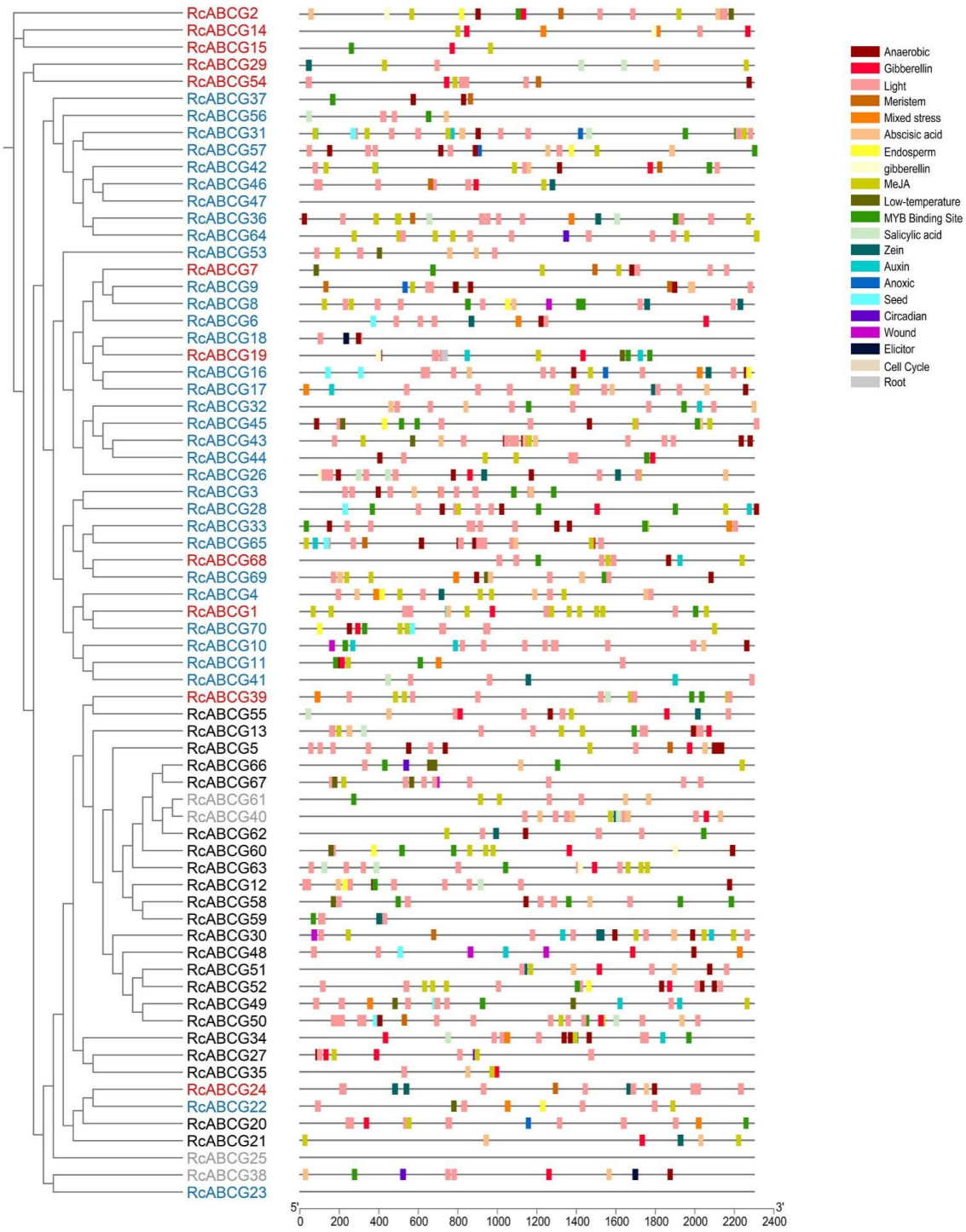

Figure 6. Cis-element analysis of the promoter of rose ABCG family genes. The type of each cis-element is indicated by colors for each *RcABCG* gene. The clustering is performed according to the results of phylogenetic analysis.

The promoter regions of seven infection-responsive full-size *RcABCG* genes, including *RcABCG5*, *RcABCG50*, *RcABCG51*, *RcABCG52*, *RcABCG58*, *RcABCG59*, and *RcABCG60*, were further examined (Supplementary Figure S3). Among them, six genes, except *RcABCG59*, contained multiple hormone- and stress-responsive elements. The promoter of *RcABCG50* contained several light-responsive, ABA-responsive, MeJA-responsive, and wound-responsive elements. MYB- and MYC-binding motifs were also detected in the promoter regions of several candidate genes, including *RcABCG50* and *RcABCG58*.

3.6. RcABCG5, RcABCG50 and RcABCG59 Were Associated with Rose Petal Resistance to B. cinerea Under VIGS Conditions

To evaluate the potential involvement of infection-responsive *RcABCG* genes in rose resistance to gray mold, four full-size transporter genes, *RcABCG5*, *RcABCG50*, *RcABCG59*, and *RcABCG60*, were selected for VIGS analysis. These genes were selected based on their infection-induced expression patterns, full-size transporter structure, successful amplification of gene-specific fragments, and phylogenetic and promoter features (Supplementary Figures S3 and S4).

Gene-specific fragments of *RcABCG5*, *RcABCG50*, *RcABCG59*, and *RcABCG60* were cloned into the pTRV2 vector, and transient silencing was performed in rose petal discs through *Agrobacterium*-mediated vacuum infiltration. RT-qPCR analysis showed that the relative transcript levels of *RcABCG5*, *RcABCG50*, *RcABCG59*, and *RcABCG60* were reduced to 22.8%, 17.9%, 35.2%, and 27.5% of the TRV-GFP control, respectively (Figure 7c–f).

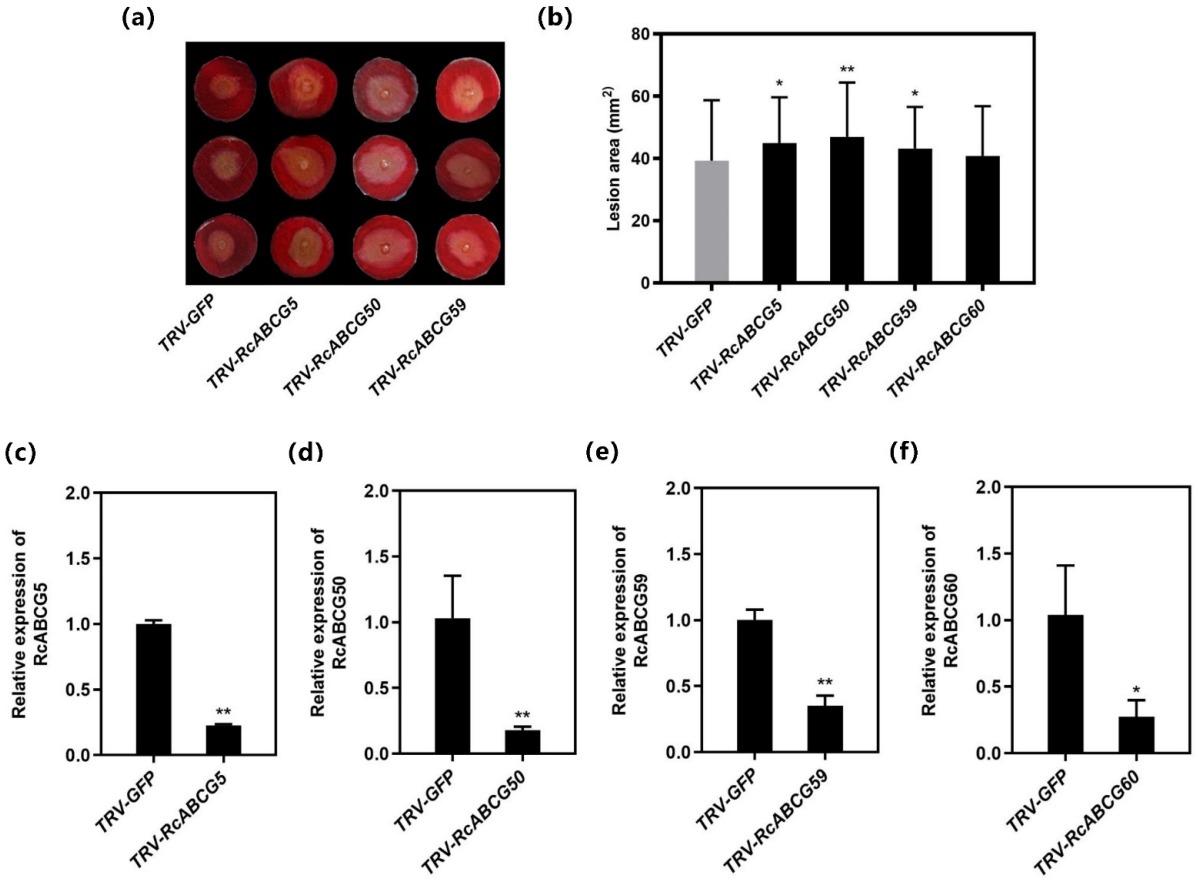

Figure 7. VIGS-based analysis of *RcABCG5*, *RcABCG50*, *RcABCG59*, and *RcABCG60* in rose petal discs after *B. cinerea* inoculation. (**a**) Disease symptoms of TRV-GFP, TRV-*RcABCG5*, TRV-*RcABCG50*, TRV-*RcABCG59*, and TRV-*RcABCG60* petal discs at 60 hpi. (**b**). Quantification of *B.cinerea* disease lesions on TRV-*RcABCG5*-, TRV-*RcABCG50*-, TRV-*RcABCG59*-, TRV-Rc*ABCG60*-, and TRV-GFP-inoculated rose petal discs. Data are shown as mean ± SD from one representative independent experiment, with at least 48 individual petal discs analyzed for each construct. (**c**) Expression of TRV-*RcABCG5* relative to that during the control at 6 days of post-silencing. (**d**) Quantification of *RcABCG50* expression in TRV-*RcABCG50*- and TRV-GFP-inoculated petal discs. (**e**) Expression of TRV-*RcABCG59* relative to that during the control at 6 days of post-silencing. (**f**) Quantification of *RcABCG60* expression in TRV-*RcABCG60*- and TRV-GFP-inoculated petal discs. The VIGS assay was independently repeated three times with similar results. Statistical significance was determined using Student's *t*-test compared with TRV-GFP. * $p < 0.05$, ** $p < 0.01$, ns, not significant. Exact *p* values are provided in the Results section.

After *B. cinerea* inoculation, larger lesion areas were observed in TRV-*RcABCG5*, TRV-*RcABCG50*, and TRV-*RcABCG59* discs compared with TRV-GFP discs. The mean lesion area was 39.27 mm^2 in TRV-GFP discs and 44.96, 46.95, and 43.23 mm^2 in *RcABCG5*-, *RcABCG50*-, and *RcABCG59*-silenced discs, respectively (Figure 7a,b). Compared with TRV-GFP, lesion areas were significantly increased in TRV-*RcABCG5* ($p = 0.0144$), TRV-*RcABCG50* ($p = 0.0015$), and TRV-*RcABCG59* ($p = 0.0381$), whereas no significant difference was observed in TRV-*RcABCG60* ($p = 0.2658$). These results suggest that *RcABCG5*, *RcABCG50*, and *RcABCG59* may contribute to rose petal resistance to *B. cinerea* under the VIGS assay conditions.

4. Discussion

Rose is an important ornamental economic crop worldwide, but gray mold caused by *B. cinerea* has become one of the most severe postharvest diseases, significantly reducing the ornamental and commercial value of roses [42,43]. The ABC transporter family plays a crucial role in the transmembrane transport of plant secondary metabolites, environmental adaptation, and defense responses [1,44]. Although ABC transporters have been extensively studied in various plant species [22], systematic identification of the ABC transporter family in rose and its functional involvement in resistance to pathogenic fungi remain limited.

In the present study, 185 *ABC* gene family members were identified in the rose genome (Table 1), a number that falls between those found in potato (54) [45] and rapeseed (314) [46]. Through phylogenetic analysis, RcABC was classified into eight subfamilies (A-G and I; Supplementary Figure S1), consistent with the classification patterns observed in Arabidopsis (129) [47], rice (133) [48], maize (133) [49], tomato (154) [50], and pepper (200) [51]. The variation in ABC transporter numbers among different plant species may reflect different degrees of gene family expansion during evolution. Notably, the RcABCG subfamily contained 70 members and represented the largest subfamily, accounting for 38% of all *RcABC* genes. Similar expansion of the ABCG subfamily has also been observed in other plant species [52]. This phenomenon may be attributed to the sessile lifestyle of plants, which necessitates the export of toxic substances and numerous secondary metabolites, many of which must be transported across membranes to reach their functional sites.

Gene duplication is an important mechanism contributing to gene family expansion. In this study, seven pairs of duplicated genes were identified within the rose *RcABC* family, and all of them belonged to the *RcABCG* subfamily (Figure 2). These duplicated gene pairs were located on different chromosomes and were classified as segmentally duplicated pairs. Ka/Ks analysis revealed that the Ka/Ks ratios of these duplicated gene pairs were consistently below 0.3 (Table 2), suggesting that these duplicated *RcABCG* genes may have undergone purifying selection during evolution. This pattern indicates that selective constraints may have contributed to maintaining conserved functions among duplicated *RcABCG* members.

ABCG subfamily transporters play important roles in plant pathogen defense by transporting defense-related metabolites and regulating hormone distribution [53]. For example, tomato SlABCG9 enhances resistance to gray mold by participating in JA synthesis and secretion [54]. In this study, DESeq2-based RNA-seq analysis identified 13 *RcABC* genes that were significantly upregulated after *B. cinerea* infection, nine of which belonged to the *RcABCG* subfamily (Table 3). This enrichment of infection-responsive genes in the *RcABCG* subfamily supports the possibility that *RcABCG* members play important roles in rose responses to gray mold infection. Phylogenetic analysis further showed that rose full-size and half-size RcABCG transporters clustered with Arabidopsis PDR and WBC transporters, respectively (Figure 4). Several previously reported defense-associated ABCG proteins were also located within branches containing full-size ABCG transporters. In addition, *RcABCG* genes with close phylogenetic relationships generally exhibited similar

exon–intron structures and conserved motif compositions (Figure 5). These results suggest that phylogenetic relationships, gene structures, and motif patterns may provide useful clues for predicting the potential functions of *RcABCG* members.

Promoter cis-acting element analysis unveiled a complex regulatory network governing *RcABCG* genes (Figure 6). Hormone-responsive elements (MeJA, ABA, gibberellin) and stress-responsive elements (anaerobic, wound) were widely distributed across *RcABCG* genes, being particularly highly enriched in candidate disease resistance genes. Notably, *ABCG* genes known to be involved in defense responses tended to cluster in the full-size transporter branch [8,11–13], and the promoter regions of these genes were enriched with MeJA, ABA, and defense-related elements. These hormones fulfill critical roles in plant resistance to gray mold: JA participates in induced defense responses, while ABA regulates stomatal closure to restrict pathogen invasion [55,56]. MYB and MYC transcription factor binding sites appeared with high frequency in multiple candidate genes (such as *RcABCG50* and *RcABCG58*), suggesting that these transcription factors may regulate the expression of *RcABCG* genes during pathogen infection through direct promoter binding.

To validate the functions of candidate genes, four full-size ABCG genes (*RcABCG5/50/59/60*) were selected for VIGS-mediated gene silencing experiments. These genes were selected based on their infection-induced expression patterns, phylogenetic relationships with defense-associated ABCG members, and the presence of hormone- and stress-responsive elements in their promoter regions. After *B. cinerea* inoculation, larger lesion areas were observed in TRV-*RcABCG5*, TRV-*RcABCG50*, and TRV-*RcABCG59* petal discs compared with TRV-GFP discs, whereas no significant difference was observed in TRV-*RcABCG60* discs (Figure 7). These results indicate that *RcABCG5/50/59* may contribute to rose resistance against gray mold. Considering the known functions of ABCG transporters in other plants, these genes may participate in rose defense responses by transporting defense-related metabolites or hormone-associated compounds, although their specific substrates remain to be identified.

There are several limitations in this study. First, the identification of *RcABC* genes was based on the current *R. chinensis* 'Old Blush' genome annotation, and some short or atypical proteins may represent incomplete annotations or truncated predictions. Therefore, further validation using improved genome assemblies or transcript evidence would help refine the *RcABC* gene set. Second, although DESeq2-based RNA-seq analysis and RT-qPCR validation supported the infection-induced expression patterns of selected *RcABC* genes, the transcriptomic analysis included only two infection time points. Additional time-course transcriptome data and broader biological conditions would provide a more comprehensive understanding of *RcABC* gene responses to *B. cinerea* infection. Third, promoter cis-element analysis provides only predictive information, and the potential regulation of *RcABCG* genes by MYB, MYC, or hormone-related transcription factors remains to be validated by approaches such as yeast one-hybrid, EMSA, dual-luciferase assays, or ChIP-qPCR. Finally, VIGS provides transient functional evidence in rose petal discs, but stable genetic transformation, overexpression analysis, and substrate transport assays are needed to further confirm the biological functions and transport mechanisms of *RcABCG5*, *RcABCG50*, and *RcABCG59*.

Overall, this study provides a genome-wide characterization of the ABC transporter family in rose and identifies *RcABCG5*, *RcABCG50*, and *RcABCG59* as candidate genes associated with *B. cinerea* resistance under VIGS conditions. These findings provide candidate genes and a useful framework for further investigation of ABCG-mediated defense mechanisms and for future molecular improvement of gray mold resistance in rose.

5. Conclusions

In summary, systematic identification and functional analysis of the rose ABC transporter family were conducted in the present study. A total of 185 *RcABC* genes were identified and classified into 8 subfamilies, with ABCG constituting the largest subfamily. Gene duplication, phylogenetic, promoter, and expression analyses indicated that *RcABCG* members may play important roles in rose responses to *B. cinerea*. VIGS-based functional assays further showed that *RcABCG5*, *RcABCG50*, and *RcABCG59* may participate in resistance to gray mold.

This study provides the first genome-wide framework for ABC transporter genes in rose and identifies defense-related *RcABCG* candidates for future functional studies and molecular breeding. Nevertheless, the present work is limited by the use of RNA-seq and transient VIGS assays, and the specific substrates transported by these *RcABCG* proteins remain to be determined. Future work should include additional time-course transcriptome analysis, stable genetic validation, overexpression analysis, transport assays, and metabolite profiling to further elucidate the mechanisms of ABCG-mediated resistance to *B. cinerea* in rose.

Supplementary Materials: The following supporting information can be downloaded at https://www.mdpi.com/article/10.3390/horticulturae12070870/s1, Supplementary Figure S1: Phylogenetic analyses of ABC protein subfamily in rose with *Arabidopsis thaliana* ABC protein family. The phylogenetic tree was constructed by MEGA7.0 using the Neighbor-joining method. Numbers on the branches represent bootstrap values. Different groups are marked with different colors. Supplementary Figure S2: (a) The sequence logos of the ABC motif in Arabidopsis thaliana. (b) The sequence logos of the ABC motif in rose. Supplementary Figure S3: Cis-element analysis of promoters of seven full-size *RcABCG* genes. Different cis-element types are indicated by different colors. Supplementary Figure S4: Homologous alignment of RcABCG50, RcABCG51, and RcABCG52 sequences. Supplementary Figure S5: Homologous alignment of RcABCG58 and RcABCG59 sequences. Supplemental Table S1: List of primers used in this study. Supplemental Table S2: MEME motifs identified in RcABCG proteins.

Author Contributions: Z.Z., X.C. and M.C. conceived this study, Z.Z. and X.L. supervised the project. X.C. and M.C. carried out experiments. X.C., H.Z. and Z.W. analyzed the data. X.C. and M.C. prepared the figures. X.C. wrote the manuscript with contributions from other co-authors. All authors have read and agreed to the published version of the manuscript.

Funding: This study was supported by the National Natural Science Foundation of China awarded to Zhao Zhang (grant numbers 32472780 and 31972444).

Data Availability Statement: The RNA-seq dataset analyzed in this study is available in the NCBI Sequence Read Archive under accession number PRJNA414570. Other data supporting the findings of this study are available from the corresponding author upon reasonable request.

Conflicts of Interest: The authors declare no conflicts of interest.

Abbreviations

VIGS, virus-induced gene silencing; *Botrytis cinerea*, *B. cinerea*; hpi, hour post inoculation; *Rosa chinensis*, *R. chinensis*; ATP-binding cassette transporters, ABC; nucleotide-binding domains, NBDs; transmembrane domains, TMDs; reactive oxygen species, ROS; Pleiotropic Drug Resistance proteins, PDRs; White-Brown Complex proteins, WBCs; gibberellic acid, GA; methyl jasmonate, MeJA; abscisic acid, ABA.

References

1. Theodoulou, F.L.; Kerr, I.D. ABC transporter research: Going strong 40 years on. *Biochem. Soc. Trans.* **2015**, *43*, 1033–1040. [CrossRef] [PubMed]

2. Furuta, T. Structural dynamics of ABC transporters: Molecular simulation studies. *Biochem. Soc. Trans.* **2021**, *49*, 405–414. [CrossRef] [PubMed]
3. Stratford, F.L.L.; Ramjeesingh, M.; Cheung, J.C.; Huan, L.J.; Bear, C.E. The Walker B motif of the second nucleotide-binding domain (NBD2) of CFTR plays a key role in ATPase activity by the NBD1-NBD2 heterodimer. *Biochem. J.* **2007**, *401*, 581–586. [CrossRef] [PubMed]
4. Do, T.H.T.; Martinoia, E.; Lee, Y.; Hwang, J.U. 2021 update on ATP-binding cassette (ABC) transporters: How they meet the needs of plants. *Plant Physiol.* **2021**, *187*, 1876–1892. [CrossRef] [PubMed]
5. Nogia, P.; Pati, P.K. Plant secondary metabolite transporters: Diversity, functionality, and their modulation. *Front. Plant Sci.* **2021**, *12*, 758202. [CrossRef] [PubMed]
6. Zhang, D.D.; Yu, Z.F.; Zeng, B.; Liu, X.Y. Genome-wide analysis of the *ABC* gene family in almond and functional predictions during flower development, freezing stress, and salt stress. *BMC Plant Biol.* **2024**, *24*, 12. [CrossRef] [PubMed]
7. Andolfo, G.; Ruocco, M.; Di Donato, A.; Frusciante, L.; Lorito, M.; Scala, F.; Ercolano, M.R. Genetic variability and evolutionary diversification of membrane ABC transporters in plants. *BMC Plant Biol.* **2015**, *15*, 51. [CrossRef] [PubMed]
8. Dhara, A.; Raichaudhuri, A. ABCG transporter proteins with beneficial activity on plants. *Phytochemistry* **2021**, *184*, 112663. [CrossRef] [PubMed]
9. Do, T.H.T.; Martinoia, E.; Lee, Y. Functions of ABC transporters in plant growth and development. *Curr. Opin. Plant Biol.* **2018**, *41*, 32–38. [CrossRef] [PubMed]
10. Li, P.; Luo, T.; Pu, X.J.; Zhou, Y.; Yu, J.N.; Liu, L. Plant transporters: Roles in stress responses and effects on growth and development. *Plant Growth Regul.* **2021**, *93*, 253–266. [CrossRef]
11. Crouzet, J.; Trombik, T.; Fraysse, A.S.; Boutry, M. Organization and function of the plant pleiotropic drug resistance ABC transporter family. *FEBS Lett.* **2006**, *580*, 1123–1130. [CrossRef] [PubMed]
12. Lee, M.; Lee, K.; Lee, J.; Noh, E.W.; Lee, Y. *AtPDR12* contributes to lead resistance in arabidopsis. *Plant Physiol.* **2005**, *138*, 827–836. [CrossRef] [PubMed]
13. Ji, H.; Peng, Y.H.; Meckes, N.; Allen, S.; Stewart, C.N.; Traw, M.B. ATP-dependent binding cassette transporter G family member 16 increases plant tolerance to abscisic acid and assists in basal resistance against *Pseudomonas syringae DC3000*. *Plant Physiol.* **2014**, *166*, 879-U618. [CrossRef] [PubMed]
14. Stein, M.; Dittgen, J.; SánChez-RodrígUez, C.; Hou, B.-H.; Molina, A.; Schulze-Lefert, P.; Lipka, V.; Somerville, S. Arabidopsis PEN3/PDR8, an ATP binding cassette transporter, contributes to nonhost resistance to inappropriate pathogens that enter by direct penetration. *Plant Cell* **2006**, *18*, 731–746. [CrossRef] [PubMed]
15. Khare, D.; Choi, H.; Huh, S.U.; Bassin, B.; Kim, J.; Martinoia, E.; Sohn, K.H.; Paek, K.-H.; Lee, Y. ABCG34 contributes to defense against necrotrophic pathogens by mediating the secretion of camalexin. *Proc. Natl. Acad. Sci. USA* **2017**, *114*, E5712–E5720. [CrossRef] [PubMed]
16. Lu, X.; Dittgen, J.; Piślewska-Bednarek, M.; Molina, A.; Schneider, B.; Svatoš, A.; Doubský, J.; Schneeberger, K.; Weigel, D.; Bednarek, P.; et al. Mutant allele-specific uncoupling of PENETRATION3 functions reveals engagement of the ATP-binding cassette transporter in distinct tryptophan metabolic pathways. *Plant Physiol.* **2015**, *168*, 814. [CrossRef] [PubMed]
17. He, Y.; Xu, J.; Wang, X.; He, X.; Wang, Y.; Zhou, J.; Zhang, S.; Meng, X. The Arabidopsis pleiotropic drug resistance transporters PEN3 and PDR12 mediate camalexin secretion for resistance to. *Plant Cell* **2019**, *31*, 2206–2222. [CrossRef] [PubMed]
18. Strader, L.C.; Bartel, B. The PLEIOTROPIC DRUG RESISTANCE8/ABCG36 ATP binding cassette transporter modulates sensitivity to the auxin precursor indole-3-butyric acid. *Plant Cell* **2009**, *21*, 1992–2007. [CrossRef] [PubMed]
19. Shiono, K.; Ando, M.; Nishiuchi, S.; Takahashi, H.; Watanabe, K.; Nakamura, M.; Matsuo, Y.; Yasuno, N.; Yamanouchi, U.; Fujimoto, M.; et al. RCN1/OsABCG5, an ATP-binding cassette (ABC) transporter, is required for hypodermal suberization of roots in rice (*Oryza sativa*). *Plant J.* **2014**, *80*, 40–51. [CrossRef] [PubMed]
20. Liorzou, M.; Pernet, A.; Li, S.; Chastellier, A.; Thouroude, T.; Michel, G.; Malécot, V.; Gaillard, S.; Briée, C.; Foucher, F.; et al. Nineteenth century French rose (*Rosa* sp.) germplasm shows a shift over time from a European to an Asian genetic background. *J. Exp. Bot.* **2016**, *67*, 4711–4725. [CrossRef] [PubMed]
21. Ullah, I.; Yuan, W.; Khalil, H.B.; Khan, M.R.; Lak, F.; Uzair, M.; Abbas, A.; Gohari, A.M.; Wu, H. Understanding infection and gray mold management: A review paper on deciphering the rose's thorn. *Phytopathol. Res.* **2024**, *6*, 42. [CrossRef]
22. Banasiak, J.; Jasinski, M. ATP-binding cassette transporters in nonmodel plants. *New Phytol.* **2022**, *233*, 1597–1612. [CrossRef] [PubMed]
23. Raymond, O.; Gouzy, J.; Just, J.; Badouin, H.; Verdenaud, M.; Lemainque, A.; Vergne, P.; Moja, S.; Choisne, N.; Pont, C.; et al. The genome provides new insights into the domestication of modern roses. *Nat. Genet.* **2018**, *50*, 772. [CrossRef] [PubMed]
24. Verrier, P.J.; Bird, D.; Buria, B.; Dassa, E.; Forestier, C.; Geisler, M.; Klein, M.; Kolukisaoglu, Ü.; Lee, Y.; Martinoia, E.; et al. Plant ABC proteins—A unified nomenclature and updated inventory. *Trends Plant Sci.* **2008**, *13*, 151–159. [CrossRef] [PubMed]

25. Lane, T.S.; Rempe, C.S.; Davitt, J.; Staton, M.E.; Peng, Y.H.; Soltis, D.E.; Melkonian, M.; Deyholos, M.; Leebens-Mack, J.H.; Chase, M.; et al. Diversity of ABC transporter genes across the plant kingdom and their potential utility in biotechnology. *BMC Biotechnol.* **2016**, *16*, 47. [CrossRef] [PubMed]
26. Larkin, M.A.; Blackshields, G.; Brown, N.P.; Chenna, R.; McGettigan, P.A.; McWilliam, H.; Valentin, F.; Wallace, I.M.; Wilm, A.; Lopez, R.; et al. Clustal W and clustal X version 2.0. *Bioinformatics* **2007**, *23*, 2947–2948. [CrossRef] [PubMed]
27. Kumar, S.; Stecher, G.; Tamura, K. MEGA7: Molecular evolutionary genetics analysis Version 7.0 for bigger datasets. *Mol. Biol. Evol.* **2016**, *33*, 1870–1874. [CrossRef] [PubMed]
28. Chen, C.J.; Wu, Y.; Li, J.W.; Wang, X.; Zeng, Z.H.; Xu, J.; Liu, Y.L.; Feng, J.T.; Chen, H.; He, Y.H.; et al. TBtools-II: A "one for all, all for one" bioinformatics platform for biological big-data mining. *Mol. Plant* **2023**, *16*, 1733–1742. [CrossRef] [PubMed]
29. Nguyen, L.T.; Schmidt, H.A.; von Haeseler, A.; Minh, B.Q. IQ-TREE: A fast and effective stochastic algorithm for estimating Maximum-Likelihood phylogenies. *Mol. Biol. Evol.* **2015**, *32*, 268–274. [CrossRef] [PubMed]
30. Kalyaanamoorthy, S.; Minh, B.Q.; Wong, T.K.F.; von Haeseler, A.; Jermiin, L.S. ModelFinder: Fast model selection for accurate phylogenetic estimates. *Nat. Methods* **2017**, *14*, 587–589. [CrossRef] [PubMed]
31. Lescot, M.; Déhais, P.; Thijs, G.; Marchal, K.; Moreau, Y.; Van de Peer, Y.; Rouzé, P.; Rombauts, S. PlantCARE, a database of plant -acting regulatory elements and a portal to tools for analysis of promoter sequences. *Nucleic Acids Res.* **2002**, *30*, 325–327. [CrossRef] [PubMed]
32. Bailey, T.L.; Johnson, J.; Grant, C.E.; Noble, W.S. The MEME Suite. *Nucleic Acids Res.* **2015**, *43*, W39–W49. [CrossRef] [PubMed]
33. Chen, C.J.; Chen, H.; Zhang, Y.; Thomas, H.R.; Frank, M.H.; He, Y.H.; Xia, R. TBtools: An integrative toolkit developed for interactive analyses of big biological data. *Mol. Plant* **2020**, *13*, 1194–1202. [CrossRef] [PubMed]
34. Wang, Y.P.; Tang, H.B.; DeBarry, J.D.; Tan, X.; Li, J.P.; Wang, X.Y.; Lee, T.H.; Jin, H.Z.; Marler, B.; Guo, H.; et al. MCScanX: A toolkit for detection and evolutionary analysis of gene synteny and collinearity. *Nucleic Acids Res.* **2012**, *40*, e49. [CrossRef] [PubMed]
35. Chen, S.F.; Zhou, Y.Q.; Chen, Y.R.; Gu, J. fastp: An ultra-fast all-in-one FASTQ preprocessor. *Bioinformatics* **2018**, *34*, 884–890. [CrossRef] [PubMed]
36. Kim, D.; Paggi, J.M.; Park, C.; Bennett, C.; Salzberg, S.L. Graph-based genome alignment and genotyping with HISAT2 and HISAT-genotype. *Nat. Biotechnol.* **2019**, *37*, 907–915. [CrossRef] [PubMed]
37. Pertea, M.; Pertea, G.M.; Antonescu, C.M.; Chang, T.C.; Mendell, J.T.; Salzberg, S.L. StringTie enables improved reconstruction of a transcriptome from RNA-seq reads. *Nat. Biotechnol.* **2015**, *33*, 290–295. [CrossRef] [PubMed]
38. Love, M.I.; Huber, W.; Anders, S. Moderated estimation of fold change and dispersion for RNA-seq data with DESeq2. *Genome Biol.* **2014**, *15*, 550. [CrossRef] [PubMed]
39. Meng, Y.L.; Li, N.; Tian, J.; Gao, J.P.; Zhang, C.Q. Identification and validation of reference genes for gene expression studies in postharvest rose flower (*Rosa hybrida*). *Sci. Hortic.* **2013**, *158*, 16–21. [CrossRef]
40. Liu, Y.L.; Schiff, M.; Dinesh-Kumar, S.P. Virus-induced gene silencing in tomato. *Plant J.* **2002**, *31*, 777–786. [CrossRef] [PubMed]
41. Cao, X.Q.; Yan, H.J.; Liu, X.T.; Li, D.D.; Sui, M.J.; Wu, J.; Yu, H.Q.; Zhang, Z. A detached petal disc assay and virus-induced gene silencing facilitate the study of resistance in rose flowers. *Hortic. Res.* **2019**, *6*, 136. [CrossRef] [PubMed]
42. Dean, R.; Van Kan, J.A.L.; Pretorius, Z.A.; Hammond-Kosack, K.E.; Di Pietro, A.; Spanu, P.D.; Rudd, J.J.; Dickman, M.; Kahmann, R.; Ellis, J.; et al. The Top 10 fungal pathogens in molecular plant pathology. *Mol. Plant Pathol.* **2012**, *13*, 414–430. [CrossRef] [PubMed]
43. Debener, T.; Byrne, D.H. Disease resistance breeding in rose: Current status and potential of biotechnological tools. *Plant Sci.* **2014**, *228*, 107–117. [CrossRef] [PubMed]
44. Yu, L.Y.; Tian, Y.J.; Wang, X.Y.; Cao, F.; Wang, H.F.; Huang, R.M.; Guo, C.L.; Zhang, H.E.; Zhang, J.Z. Genome-wide identification, phylogeny, evolutionary expansion, and expression analyses of ABC gene family in Castanea mollissima under temperature stress. *Plant Physiol. Bioch.* **2025**, *219*, 109450. [CrossRef] [PubMed]
45. Zaynab, M.; Wang, Z.K.; Hussain, A.; Bahadar, K.; Sajid, M.; Sharif, Y.; Azam, M.; Sughra, K.; Raza, M.A.; Khan, K.A.; et al. ATP-binding cassette transporters expression profiling revealed its role in the development and regulating stress response in *Solanum tuberosum*. *Mol. Biol. Rep.* **2022**, *49*, 5251–5264. [CrossRef] [PubMed]
46. Zhang, X.D.; Zhao, K.X.; Yang, Z.M. Identification of genomic ATP binding cassette (ABC) transporter genes and Cd-responsive ABCs in. *Gene* **2018**, *664*, 139–151. [CrossRef] [PubMed]
47. Sánchez-Fernández, R.; Davies, T.G.E.; Coleman, J.O.D.; Rea, P.A. The ABC protein superfamily, a complete inventory. *J. Biol. Chem.* **2001**, *276*, 30231–30244. [CrossRef] [PubMed]
48. Garcia, O.; Bouige, P.; Forestier, C.; Dassa, E. Inventory and comparative analysis of rice Arabidopsis ATP-binding cassette (ABC) systems. *J. Mol. Biol.* **2004**, *343*, 249–265. [CrossRef] [PubMed]
49. Pang, K.Y.; Li, Y.J.; Liu, M.H.; Meng, Z.D.; Yu, Y.L. Inventory and general analysis of the ATP-binding cassette (ABC) gene superfamily in maize (*Zea mays* L.). *Gene* **2013**, *526*, 411–428. [CrossRef] [PubMed]
50. Ofori, P.A.; Mizuno, A.; Suzuki, M.; Martinoia, E.; Reuscher, S.; Aoki, K.; Shibata, D.; Otagaki, S.; Matsumoto, S.; Shiratake, K. Genome-wide analysis of ATP binding cassette (ABC) transporters in tomato. *PLoS ONE* **2018**, *13*, e0200854. [CrossRef] [PubMed]

51. Lopez-Ortiz, C.; Dutta, S.K.; Natarajan, P.; Peña-Garcia, Y.; Abburi, V.; Saminathan, T.; Nimmakayala, P.; Reddy, U.K. Genome-wide identification and gene expression pattern of ABC transporter gene family in *Capsicum* spp. *PLoS ONE* **2019**, *14*, e0215901. [CrossRef] [PubMed]
52. Zhang, D.; Hu, Y.Y.; Tang, L.; Du, Y.X.; Mao, R.H.; Sheng, X.B.; Liu, H.M.; Liu, X.L.; Zhao, B.R.; Lei, D.Y. ABCG transporters in the adaptation of rice to salt stresses. *Int. J. Mol. Sci.* **2024**, *25*, 10724. [CrossRef] [PubMed]
53. Gupta, B.B.; Selter, L.L.; Baranwal, V.K.; Arora, D.; Mishra, S.K.; Sirohi, P.; Poonia, A.K.; Chaudharya, R.; Kumar, R.; Krattinger, S.G.; et al. Updated inventory, evolutionary and expression analyses of G, (PDR) type ABC transporter genes of rice. *Plant Physiol. Bioch.* **2019**, *142*, 429–439. [CrossRef] [PubMed]
54. Tao, N.; Liu, Y.H.; Zhang, B.; Guo, Y.; Wang, Q.G.; Li, Q.Q. SlABCG9 functioning as a jasmonic acid transporter influences tomato resistance to *Botrytis cinerea*. *J. Agr. Food Chem.* **2025**, *73*, 3897–3907. [CrossRef] [PubMed]
55. Wang, Q.Y.; Chen, X.L.; Chai, X.F.; Xue, D.Q.; Zheng, W.; Shi, Y.Y.; Wang, A.X. The involvement of jasmonic acid, ethylene, and salicylic acid in the signaling pathway of *Clonostachys rosea* -induced resistance to gray mold disease in tomato. *Phytopathology* **2019**, *109*, 1102–1114. [CrossRef] [PubMed]
56. Yu, Y.Y.; Si, F.J.; Wang, N.; Wang, T.; Jin, Y.; Zheng, Y.; Yang, W.; Luo, Y.M.; Niu, D.D.; Guo, J.H.; et al. *Bacillus*-secreted oxalic acid induces tomato resistance against gray mold disease caused by activating the JA/ET pathway. *Mol. Plant-Microbe Interact.* **2022**, *35*, 659–671. [CrossRef] [PubMed]